

Quality control test for electronic portal imaging device using QC-3 phantom with PIPSPRO

Birendra Kumar Rout^{1,2}, Mukka Chandra Shekar², Alok Kumar³, Kondapalli Kesava Durga Ramesh⁴

¹Department of Radiation Physics, Aditya Birla Memorial Hospital, Pune, India

²Department of Physics, Jawaharlal Nehru Technological University, Hyderabad, India

³Department of Radiation Physics, Mahavir Cancer Sansthan, Patna, India

⁴Department of Radiation Oncology, Navodaya Cancer Institute & Research Center, Bhopal, India

Received July 10, 2014; Revised August 23, 2014; Accepted September 18, 2014; Published Online September 29, 2014

Original Article

Abstract

Purpose: A Quality control (QC) test suitable for routinely daily use has been established for electronic portal imaging device (EPID) using PIPSPRO software, version 4.4. It provides an objective and quantitative test for tolerable image quality on the basis of the high contrast spatial resolution, the contrast-to-noise ratio (CNR) and noise. **Methods:** The test uses a QC-3 phantom consisting of five sets of high contrast rectangular bar patterns with spatial frequencies of 0.10, 0.20, 0.25, 0.43 and 0.75 lp/mm using 6MV and 15MV photon energy for acquiring high quality images. A “base line” value for the relative square wave modulation transfer function (RMTF), CNR and Noise data was obtained during a one week calibration period and one month test period. **Results:** Subsequent measurements shows significant deviations from baseline values, resulting in warning messages “potential problems in system performance”. The QC test uses high contrast spatial resolution and CNR for the system with acceptable performance. **Conclusion:** The method provides an automatic, objective, and sensitive measure of the system's imaging performance. This is a useful implementation during acceptance testing, commissioning, and routine quality control.

Keywords: EPID; QC-3 Phantom; PIPSPRO; Spatial Resolution; CNR; Noise

Introduction

Verification of the field placement is an indispensable part of a compressive quality assurance program for radiation oncology. Task group (TG) report¹ suggested by American Association of Physicists in Medicine (AAPM) recommends for acquiring portal images at least once in a week, which is frequently used in most of the clinical practices. With the recent expansion of electronic portal devices² (EPID), verification is now much simpler and could be carried out on a more frequent basis with the expectation of reducing gross field placement errors and increasing overall treatment accuracy.

However, the effectiveness of an EPID depends mostly on the image quality of the device to verify patient set-up and positioning prior to radiation therapy treatments.³ Hence, it is equally important for device itself to maintain in its design and devise quality control (QC) tests to boost better image quality. These tests are essential by the manufacture at design, manufacture, operation, installation and by the user, all the way through the lifetime of the equipment. Nevertheless, as these systems are the part of regular clinical practice, it is very important to ensure the correct and reliable opera-

tion of systems at all times. Lutz^{4,5} and the Las Vegas^{6,7} phantoms has been reported to check the accuracy and the image quality for the qualitative visual QA checks of patient imaging.⁸

Here in, we report a less subjective approach for automatic daily quality control tests to get better image quality for patient. In a study presently underway at our institute, an integrated EPID-based QA system is being developed, which aims to replace the conventional device-dependent methods for daily and monthly QA tasks. In light of that, this investigation reports on the image quality, relative modulation transfer function, critical frequency and contrast-to-noise ratio obtained.

Methods and Materials

QC-3 PHANTOM

The QC-3(Standard Imaging, Middleton, WI) phantom is used to test the image quality from EPIDs. Megavoltage portal images are acquired with the phantom placed on the sur-

face of an EPID at source-to-detector distance (SDD) 140 cm. The position of phantom can be at different distances such as 160 cm, 150 cm or at isocenter but need to maintain same distance always. A QC-3 phantom was designed for use in the test, which consists of five sets of high-contrast rectangular bars with spatial frequencies of 0.10, 0.20, 0.25, 0.43, and 0.75 lp/mm and dimensions of $13.5 \times 11.3 \times 3.6$ cm³. A schematic diagram of the QC phantom is shown in **Figure 1 (a)**. The diagram shows the numbered regions of phantom QC-3. The large numbers in the corners are used for subjective quality control, as they are visible on the image with increasing density as (Number 1 is machined into a lead block to a depth of 1 mm, number 2 to a depth of 2 mm, etc.).

The small numbers indicate the region numbers. Regions 1 - 5 are bars with different spatial separations, and are used for the analysis of the spatial resolution f_{50} . Regions 6 - 11 contain blocks of lead or plastic (PVC) with increasing thicknesses. With the EPID located under the patient (0° in the Varian gantry coordinate systems), the phantom is placed on the top of the EPID detector housing in order to acquire test images. We prefer this location rather than the isocenter to minimize blurring due to the beam penumbra, since the test is intended to monitor the performance of the EPID and should be independent of the linac source size. The phantom is rotated to 45° relative to the EPID scan lines to prevent aliasing in the image of the bar patterns.

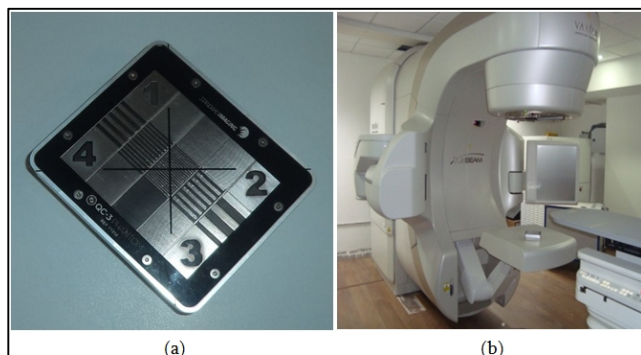


FIG. 1(a) and 1(b): Image of the QC-3 phantom from standard imaging; and phantom position during taking image.

aS1000 EPID

The Varian aS1000 (Portal Vision, Varian Medical Systems, Palo Alto, CA) is an amorphous silicon flat panel imaging device mounted on a robotic arm. It has an active imaging area of 40×30 cm² (at an SSD of 105 cm). The image matrix is created from an array of 1024×768 pixels. The maximum frame acquisition rate is 9.574 frames/second, the permitted energy range is 4 - 25 MV, and the permitted dose rates are 50 - 600 MU/min. The detector has four main components. Inside the exterior plastic housing there is a Copper build-up plate, 1 mm in thickness. This is useful in MV imaging to absorb x-ray photons and emit recoil electrons. It also helps

to improve the efficiency of the entire imaging system, by partially shielding the downstream components (including the scintillation screen) from scattered radiation. Underneath this plate lies the phosphor screen. In this EPID it is a Kodak Lanex Fast B scintillating screen, made up of a 0.4 mm thick Gadolinium Oxysulfide (Gd₂O₂S: Tb) phosphor.

This component absorbs the recoil electrons coming from the Copper plate, and transforms them into visible light. Below the phosphor, there is a 1024×768 pixel matrix, deposited on a 1 mm glass substrate. This constitutes the sensitive image forming layer of the photodiode system, and it is 1.5 μm thick. Each pixel consists of a Si n-i-photodiode to integrate the incoming light in charge captures and a thin film transistor (TFT) to act as a three-terminal switch for readout. The final major component is the accessory electronics, which drive the TFT switches and read out the charge captures. The gate driver powers the gate lines during the time that the data lines are feeding the accumulated charge to the read-out electronics.

When a voltage is applied to a gate-line, all of the TFTs in that row become transparent and the charge is then transferred to the data lines. Each row is read out in succession, and as one row is read the TFTs in the next row become transparent. External charge sensitive amplifiers capture the charge data. To form one frame of an image, a sequential readout of all of the rows is necessary.

Before each set of EPID images is acquired it is advisable to first calibrate the detector. This can be accomplished by obtaining a dark field and delivering a flood field. The premise is that taking these images will allow for the elimination of background noise and provide a uniform response for imaging. Specifically, the dark field image provides information about background noise, and is obtained by reading out each pixel in the absence of radiation. The resulting image, seen in, is a series of narrow vertical stripes, which result from the photodiode leakage current and varying electrometer offsets. The flood field image, on the other hand, is taken with the entire matrix exposed to a uniform dose. This allows the Portal Vision software to internally correct for individual pixel sensitivities. There is much to say about the acquisition and use of these images inside the Portal Vision software package.

Acquiring QC Images

The phantom is setup on the EPID at 140 cm, oriented at 45° to the sagittal plane, as shown in the **Figure 1(b)**. The large number 1 points towards the gantry. Lines and marks on the surface of the phantom assist in lining it up to the central beam line. For routine daily or weekly quality control, it is advisable to mark the surface of the EPID with paint or tape so that placement of the phantom can be done quickly. A stand is available for lateral imaging. Two images of the

phantom are acquired under identical conditions, preferable during the same irradiation sequence. The obtained images were transferred to the PIPSPRO software for analysis.

The analysis program places a region of interest (ROI) over each set of bars as shown in **Figure 2**. The frequency dependent square wave modulation transfer function (SWMTF) is determined by the method proposed by Droegge⁹ and the frequency for 50% modulation (f_{50}) is compared with the predetermined critical frequency f_c as a test of system performance.

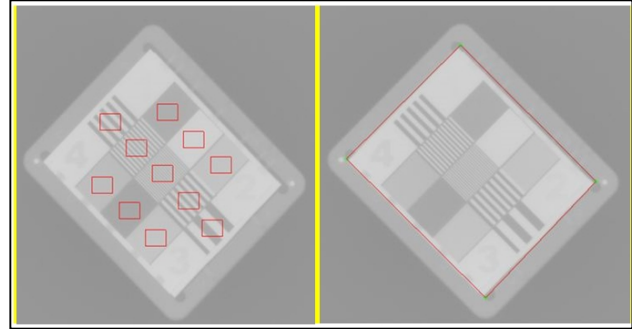


FIG. 2: A portal image of the QC phantom at diagonal orientation obtained with the aS1000 portal imaging system. The ROIs used for the QC test are marked on the image.

TABLE 1: Mean value of f_{30} , f_{40} , f_{50} , CNR and noise measured at gantry angle 0° for both 6MV and 15MV phantom is physically displaced relative to the beam center by each of the four directions in a plane orthogonal to the beam.

| SL No | Parameter | 6MV | | | | | 15MV | | | | |
|-------|---------------|----------|----------|----------|---------|-------|----------|----------|----------|---------|--------|
| | | f_{30} | f_{40} | f_{50} | CNR | Noise | f_{30} | f_{40} | f_{50} | CNR | Noise |
| 1 | Without shift | 0.74 | 0.602 | 0.463 | 192.636 | 9.82 | 0.603 | 0.457 | 0.365 | 170.634 | 9.916 |
| 2 | 5°Left | 0.739 | 0.599 | 0.46 | 192.376 | 9.754 | 0.6 | 0.452 | 0.362 | 170.35 | 9.868 |
| 3 | 5° RT | 0.742 | 0.605 | 0.468 | 189.666 | 9.795 | 0.611 | 0.467 | 0.371 | 167.146 | 9.886 |
| 4 | 1 CM IN | 0.734 | 0.6 | 0.467 | 194.526 | 9.753 | 0.604 | 0.462 | 0.367 | 169.996 | 9.974 |
| 5 | 1CM OUT | 0.745 | 0.605 | 0.464 | 189.15 | 9.918 | 0.605 | 0.456 | 0.366 | 173.23 | 9.748 |
| 6 | 1CM LEFT | 0.741 | 0.603 | 0.465 | 191.173 | 9.846 | 0.606 | 0.46 | 0.367 | 167.544 | 9.947 |
| 7 | 1CM RT | 0.734 | 0.596 | 0.457 | 192.107 | 9.825 | 0.601 | 0.453 | 0.364 | 166.318 | 10.048 |

TABLE 2: Mean values and standard deviation of f_{30} , f_{40} , f_{50} , CNR and noise measured at gantry angle 0° over 40 days (7 days calibration period and 33 days test period) for both 6MV and 15MV Values and standard deviations are rounding up to 3 digits.

| Parameters | 6MV Photon energy | | 15MV Photon energy | |
|------------|--------------------|--------------------|--------------------|--------------------|
| | During calibration | During Test period | During calibration | During Test period |
| f_{50} | 0.463± 0.003 | 0.464± 0.003 | 0.365± 0.001 | 0.366± 0.001 |
| f_{40} | 0.602± 0.003 | 0.602± 0.001 | 0.457± 0.002 | 0.458± 0.003 |
| f_{30} | 0.741± 0.002 | 0.741± 0.002 | 0.603± 0.002 | 0.605± 0.003 |
| CNR | 192.636±1.348 | 191.293±2.192 | 170.634±1.464 | 170.013±1.734 |
| Noise | 9.82±0.094 | 9.866±0.109 | 9.916±0.135 | 9.931±0.122 |

Determination of the RMTF

The SWMTF of an imaging system is defined as

$$SWMTF(f) = \Delta E(f) / \Delta E_0$$

Where ΔE_0 and $\Delta E(f)$ are the modulations of input to and output from the system. Since we are not interested in the absolute measure of the SWMTF, but only in determine day to-day variations in the system resolution, we use a relative measure¹⁰ (RMTF) of the SWMTF by calculating:

$$RMTF(f) = \Delta E(f) / \Delta E(f_1)$$

Or, $RMTF(f) = MTF(f) / MTF(0.1LP/mm)$

where, $\Delta E(f_1)$ is the output modulation for the lowest frequency.

Usually the output modulation $\Delta E(f)$ is difficult to obtain from a noisy image; therefore, Droge and Morin¹¹ suggest

using the relationship between signal amplitude and its variance. For sinusoidal output, $(\Delta E)^2$ is proportional to the Variance $(M)^2$ within the ROI containing the bar pattern, and the above relation can be written as

$$RMTF(f) = M(f) / M(f_1)$$

In the presence of random image noise (f) can be obtained by

$$M^2(f) = \sigma_m^2(f) - \sigma^2(f)$$

where, $\sigma_m^2(f)$ and $\sigma^2(f)$ are the measured total variance and the variance due to random noise, respectively. The total variance $\sigma_m^2(f)$ is obtained by measuring the variance of the pixel in the ROI corresponding the frequency f . In order to measure the random noise in an image, a pair of similar images are subtracted, and the standard deviation is obtained from the difference, thus avoiding contributions from fixed pattern noise. In this case, the variance of the subtracted ROI (σ_{sub}^2) will be

$$\sigma_{sub}^2 = \sigma_1^2 + \sigma_2^2$$

where, σ_1^2 and σ_2^2 are the random noise variance of the ROIs for each image. We assume that these two variance are equal and hence;

$$\sigma_1 = \sigma = \sigma_{\text{sub}} / \sqrt{2}$$

The variance σ^2 (f) is calculated once using above equation for the set of bars with the highest frequency (0.75 lp/mm) on the assumption that random noise is same for all ROIs.

Critical Frequency (f_{50})

Critical frequency is defined as the spatial resolution corresponding to 50% RMTF. This value is obtained using a piecewise linear interpolation of the RMTF graph to locate the 50% relative frequency response. (f_{40}) is defined as the spatial resolution corresponding to 40% maximum of the relative modulation transfer function (RMTF). f_{30} is defined as the spatial resolution corresponding to 30% maximum of the relative modulation transfer function RMTF.

Contrast-to-Noise Ratio

A high quality image typically has a large CNR. This can be manipulated by increasing the Contrast, decreasing the noise, or a combination of both. CNR is defined by the following equation:

$$\text{CNR} = \frac{P_{\text{bright}} - P_{\text{dark}}}{\text{Noise}}$$

where, P_{bright} is the average pixel value in the areas receiving the least radiation, P_{dark} is the average pixel value in the areas receiving the most radiation dose, and Noise represents the average noise value calculated from the uniformly irradiated regions.

Phantom Alignment

Electronic portal Imaging systems utilize non-square pixels giving rise to different MTFs in horizontal and vertical directions. By using the diagonal phantom orientation, a combine measure of resolution in both directions could be obtained, as well as reduction in error due to possible changes in ROI size and positioning.⁹ RMTF (f) were exhaustively tested against changes in the ROI size and position. Images are acquired with a 6MV and 15MV photon beams when the phantom was physically displaced relative to the beam center by each of the four directions in a plane orthogonal to the beam. Changes in f_{50} and CNR were 0.86% and 0.72% respectively for 6MV and 0.27% and 0.8% for 15MV. Rotating the phantom by $\pm 5^\circ$ from the correct 45° angle introduced changes in f_{50} and CNR of 0.22% and 0.82% respectively for 6MV and 0.27% and 1.12% for 15MV.

This displacement and rotations are much larger than any anticipated in normal use of the phantom for routine quality control measurements as mentioned in Table-1. The complete QC procedure was tested by repeating daily for 7 consecutive days. Deliberately moving the ROIs by two pixels (about 1.2mm at isocenter) to the left, right, up and down gave change in f_{50} and CNR of less than 0.3% and 1.1%, respectively. Changing the field size and increasing the image acquisition times did not have a significant influence on the measured results.

Results

Measurements were made daily on the EPID imaging system with dual-energy linear accelerator by using 6MV and 15MV photons to 3-5 MU at images for high quality images distance with SDD 140 cm. System performances was monitored during a test period of 1 month and these data were used to determine the mean and standard deviation of f_{50} , f_{40} and f_{30} .

Before the QC needs to established Base line values for resolution, CNR and noise, after calibration of imager a series of one QC tests per day over the first one week. "base line" value is shown (**Figure 3**) by the blue line in PIPSPRO software. The green area is within the acceptable parameters, the yellow area represents the caution levels, and the red areas represent the reject levels. Suggested values for accept and caution ranges are 5 and 10 percent respectively for all values except noise where 10 and 20 percent is suggested due to the fact that noise tends to fluctuate more than the other parameters.

During the one week calibration the mean values of f_{50} , f_{40} and f_{30} (\pm standard deviation) were 0.463 ± 0.003 , 0.602 ± 0.003 and 0.741 ± 0.002 respectively for 6MV. The mean values of f_{50} , f_{40} and f_{30} (\pm standard deviation) were 0.365 ± 0.001 , 0.457 ± 0.002 and 0.603 ± 0.002 respectively for 15MV. The mean value of CNR and Noise were 192.636 ± 1.348 , 9.82 ± 0.094 for 6MV and 170.634 ± 1.464 , 9.916 ± 0.135 for 15MV respectively. **Figure 4 and Figure 5** shows f_{50} and CNR a plot of recorded on a daily basis for the as1000 system which included one month QC data for both high and low energy. The mean values of f_{50} , f_{40} and f_{30} (\pm standard deviation) were 0.464 ± 0.003 , 0.602 ± 0.001 and 0.741 ± 0.002 respectively for 6MV. The mean values of f_{50} , f_{40} and f_{30} (\pm standard deviation) were 0.366 ± 0.001 , 0.458 ± 0.003 and 0.605 ± 0.003 respectively for 15MV. The mean value of CNR and Noise were 191.293 ± 2.192 , 9.866 ± 0.109 for 6MV and 170.013 ± 1.734 , 9.931 ± 0.122 for 15MV respectively as mentioned in the **Table 2**.

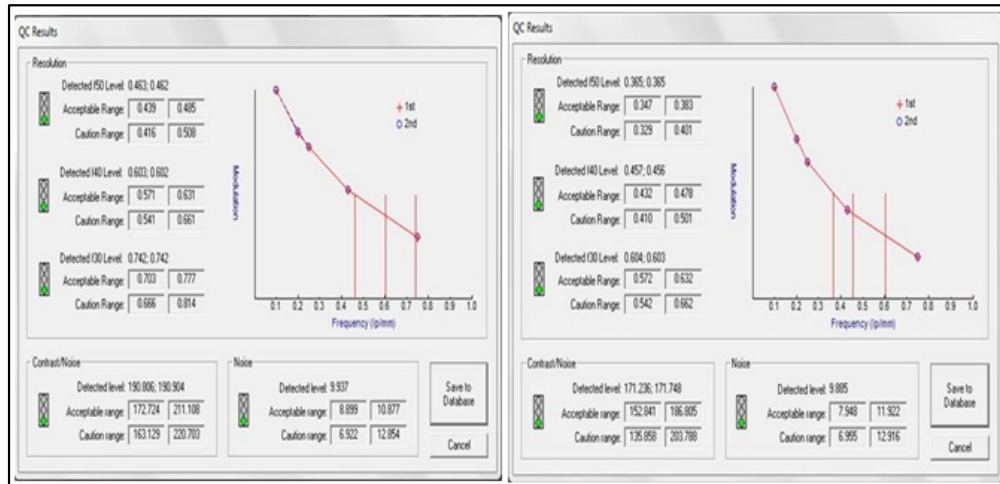


FIG. 3: RMTF curves, created using the PIPspro Software. The 6mv curve is in left, and the 15MV curve is on the right.

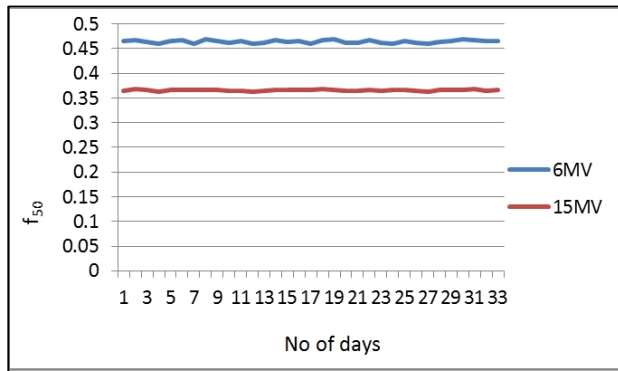


FIG. 4: Plot of f_{50} recorded on a daily basis for the as1000 portal imaging system with gantry angle 0° at 6MV and 15MV.

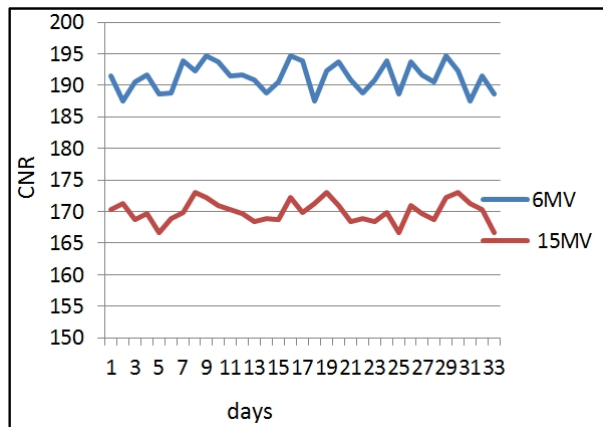


FIG. 5: Plot of CNR recorded on a daily basis for the as 1000 portal imaging system with gantry angle 0° at 6MV and 15MV.

It is seen that system resolution at 6MV is superior to that 15 MV, an effect which has been observed previously and is a result of the larger physical beam penumbra at higher energies^{12, 13, 14} and increased transmission through the bar patterns by the higher energy photons. It is seen that CNR for 6MV is

higher than that for 15MV. Gantry angle at 90° also checked during the one week calibration for both 6MV and 15MV. The mean values of f_{50} , f_{40} and f_{30} (\pm standard deviation) were 0.459 ± 0.007 , 0.462 ± 0.018 and 0.684 ± 0.022 for 6MV (Figure 6). The mean values of f_{50} , f_{40} and f_{30} (\pm standard deviation) were 0.421 ± 0.012 , 0.531 ± 0.016 and 0.645 ± 0.019 for 15MV. The mean value of CNR and Noise were 203.05 ± 1.923 , ± 0.085 for 6MV and 162.528 ± 1.822 , 9.399 ± 0.078 for 15MV respectively (Figure 7).

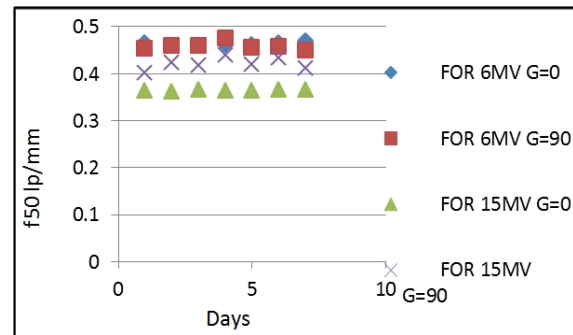


FIG. 6: Plot of f_{50} recorded on a daily basis for the as1000 portal imaging system with Gantry Angle 0° and 90° at 6MV and 15MV for days.

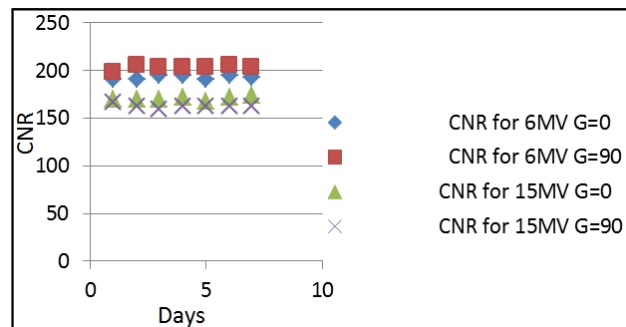


FIG. 7: Plot of f_{50} recorded on a daily basis for the as1000 portal imaging system with Gantry Angle 0° and 90° at 6MV and 15MV for 7 days.

Discussion

According to Task Group 142 report¹⁵: Quality assurance of medical accelerator, spatial resolution, Contrast, uniformity and noise should match to base line. In our case deviation of f_{50} CNR and noise were 0.22%, 0.70% and 0.47 for 6MV and 0.27%, 0.36% and 0.15 % respectively for 15MV from Base line which is meeting excellently. Quantitatively, specification value for Varian aS1000 f_{50} was 0.45 for 6MV and 0.379 for 10-25 MV. In our case spatial Resolution f_{50} for 6MV is 0.463 ± 0.003 and 0.365 ± 0.001 for 15MV which is very close to given data. Deviation for 6MV and 15MV were 2.2% and 3.4%, respectively. Spatial resolution of f_{40} and f_{30} following the f_{50} in proper sequence. The mean values of f_{50} , f_{40} , f_{30} (\pm standard deviation), CNR and noise excellently matching for both during the calibration period and test period for both of 6MV and 15MV.

Conclusion

We have established a QC test for portal imaging devices suitable for routine daily use for testing the system for acceptable performance in high contrast spatial resolution and CNR. It is shown that this method provides an automatic, objective, and sensitive measure of the system's imaging performance and it is useful tool during acceptance testing, commissioning, and routine quality control.

Conflict of interest

The authors declare that they have no conflicts of interest. The authors alone are responsible for the content and writing of the paper.

References

1. Kutcher GJ, Coia L, Gillin M, *et al.* Comprehensive QA for radiation oncology: report of AAPM Radiation Therapy Committee Task Group 40. *Med Phys* 1994; **21**:581-618.
2. Boyer AL, Antonuk L, Fenster A, *et al.* A review of electronic portal imaging devices (EPIDs). *Med Phys* 1992; **19**:1-16.
3. Verellen D, De Neve W, Van den Heuvel F, *et al.* On-line portal imaging: image quality defining parameters for pelvic fields--a clinical evaluation. *Int J Radiat Oncol Biol Phys* 1993; **27**:945-52.
4. Lutz WR, Bjarngard BE. A test object for evaluation of portal films. *Int J Radiat Oncol Biol Phys* 1985; **11**:631-4.
5. Leszczynski KW, Shalev S. Digital contrast enhancement for online portal imaging. *Med Biol Eng Comput* 1989; **27**:507-12.
6. Wong JW, Cheng AY, Binns WR, *et al.* Development of a second-generation fiber-optic on-line

image verification system. *Int J Radiat Oncol Biol Phys* 1993; **26**:311-20.

7. Herman MG, Abrams RA, Mayer RR. Clinical use of on-line portal imaging for daily patient treatment verification. *Int J Radiat Oncol Biol Phys* 1994; **28**:1017-23.
8. Murthy KK, Al-Rahbi Z, Sivakumar SS, *et al.* Verification of set up errors in external beam radiation therapy using electron portal imaging. *Med Phys* 2008; **33**:49-53.
9. Droege RT. A practical method to routinely monitor resolution in digital images. *Med Phys* 1983; **10**:337-43.
10. Arimura H, Kubota H, Matsumoto M, *et al.* Wiener spectra of quantum mottle and the squares of modulation transfer function. *Phys Med Biol* 1999; **44**:1337-52.
11. Droege RT, Morin RL. A practical method to measure the MTF of CT scanners. *Med Phys* 1982; **9**:758-60.
12. Wowk B, Radcliffe T, Leszczynski KW, Shalev S, Rajapakshe R. Optimization of metal/phosphor screens for on-line portal imaging. *Med Phys* 1994; **21**:227-35.
13. Munro P, Rawlinson JA, Fenster A. Therapy imaging: a signal-to-noise analysis of a fluoroscopic imaging system for radiotherapy localization. *Med Phys* 1990; **17**:763-72.
14. Rajapakshe R, Luchka K, Shalev S. A quality control test for electronic portal imaging devices. *Med Phys* 1996; **23**:1237-44.
15. Klein EE, Hanley J, Bayouth J, *et al.* Task Group 142 report: quality assurance of medical accelerators. *Med Phys* 2009; **36**:4197-212.